

Influence Maximization in Temporal Networks with Persistent and Reactive Behaviors

Aaqib Zahoor *, Iqra Altaf Gillani, and Janib ul Bashir

Department of Information Technology, NIT Srinagar, India

{aaqib_phaite003, iqraaltaf, janibbashir}@nitsri.ac.in

Abstract

Influence maximization in temporal social networks presents unique challenges due to the dynamic interactions that evolve over time. Traditional diffusion models often fall short in capturing the real-world complexities of active-inactive transitions among nodes, obscuring the true behavior of influence spread. In dynamic networks, nodes do not simply transition to an active state once; rather, they can oscillate between active and inactive states, with the potential for reactivation and reinforcement over time. This reactivation allows previously influenced nodes to regain influence potency, enhancing their ability to spread influence to others and amplifying the overall diffusion process. Ignoring these transitions can thus conceal the cumulative impact of influence, making it essential to account for them in any effective diffusion model. To address these challenges, we introduce the Continuous Persistent Susceptible-Infected Model with Reinforcement and Re-activation (cpSI-R), which explicitly incorporates active-inactive transitions, capturing the progressive reinforcement that makes nodes more potent spreaders upon reactivation. This model naturally leads to a submodular and monotone objective function, which supports efficient optimization for seed selection in influence maximization tasks. Alongside cpSI-R, we propose an efficient temporal snapshot sampling method, simplifying the analysis of evolving networks. We then adapt the prior algorithms of seed selection to our model and sampling strategy, resulting in reduced computational costs and enhanced seed selection efficiency. Experimental evaluations on diverse datasets demonstrate substantial improvements in performance over baseline methods, underscoring the effectiveness of cpSI-R for real-world temporal networks.

1 Introduction

Social networks have become critical platforms for disseminating information, as more individuals express their opinions online. Understanding how influence and information flow through these networks has emerged as a key area of research. One common example is businesses leveraging “word of mouth” marketing to promote new products on social networks. To achieve this, they identify a small group of early adopters or “seeds,” whose acceptance of the product will trigger widespread adoption through social influence. This process, known as influence maximization (IM), focuses on selecting the most influential seed users to maximize the spread of information or influence.

The challenge of influence maximization lies in identifying those initial users (seeds) who are likely to influence the largest number of others. The objective is to select these seeds to maximize the expected number

*Corresponding Author

of eventual adopters, given a social network and a limited number of seed users. Kempe et al. [1] first introduced this problem, and since then, it has been widely studied, particularly in viral marketing applications [2]. Over time, various advancements have been made, including methods for measuring influence size, adaptive seeding techniques, and increasing seeding efforts [3][4][5][6].

At the core of influence maximization is estimating the expected number of users influenced by different seed sets, typically by considering each user’s probability of activation. This activation probability reflects the likelihood that a user will influence their neighbors after being influenced. While many existing methods are adept at identifying influential seed users, they often assume a static network structure. This assumption fails to capture the dynamic and ever-evolving nature of real-world social networks. Recent studies have focused on addressing this limitation in online settings [7][8][9][10], yet the challenge of ensuring optimal seed selection in temporal networks remains. In most cases, the spread function becomes non-monotone and non-submodular, complicating optimization. Additionally, traditional models like Independent Cascade (IC), Linear Threshold (LT), SI, and SIR fail to account for the persistence and reactivation of nodes, assuming once a node is activated, it cannot re-engage. This overlooks the evolving dynamics of influence in real-world networks. In reality, influence spread is not a one-time event; it evolves as individuals interact with new content or developments. For example, a user initially influenced by a campaign post might later re-engage after seeing a new post, update, or comment. This re-engagement can be sparked by various factors, such as a trending hashtag, a viral video, or a new political debate that reignites interest in the campaign’s message.

Consider a scenario where a major political debate draws attention. Users who were previously inactive may become active again, resharing old posts or creating new content in support of a candidate. Similarly, a controversy involving a competitor could lead to increased activity as users re-engage with the campaign, amplifying its message to take advantage of shifting public sentiment. This ongoing cycle of engagement and re-engagement, driven by trends and events, reflects the complex nature of influence dynamics in social networks. Unlike traditional diffusion models, which assume influence is static, these examples illustrate how influence can persist and evolve over time as users interact with new information. Understanding these dynamic interactions is essential for developing effective influence maximization strategies that can adapt to changing social media landscapes. To address these challenges, this paper critically examines the limitations of traditional diffusion models, which often render the objective function non monotone and non submodular with no impact on effectively capturing the real-world dynamics of temporal graphs. Building on this analysis, we introduce the Continuous Persistent Susceptible-Infected Model with Reinforcement and Re-activation (cpSI-R), a novel approach that achieves more accurate modeling of influence spread in temporal social networks. The cpSI-R model improves upon traditional diffusion frameworks by incorporating mechanisms for node reactivation and persistent influence through reinforcement. This allows nodes to continue exerting influence even after their initial activation, providing a more realistic representation of influence dynamics in evolving networks. Furthermore, the cpSI-R model preserves the desirable properties of monotonicity and submodularity in the spread function, enabling efficient optimization algorithms. Building on the cpSI-R model, we propose a new influence maximization algorithm based on the forward influence algorithm [11], enhanced with an efficient sampling method that captures temporal snapshots of the network. By discretizing time intervals based on structural changes in the network, our approach ensures highly accurate computation of the influence spread from the selected seed nodes. The problem therefore can be stated as:

Problem 1. *Given a temporal network $G = (V, E)$ with nodes V and edges E , and a diffusion model defined by the Continuous Persistent Susceptible-Infected Model with Time-Limited Reinforcement and Re-activation (cpSI-R), the goal is to select an initial set $S \subseteq V$ of nodes at time t_0 to maximize the spread of infection by time $t_0 + h$. Formally, let $\sigma(S, t_0, t_0 + h)$ denote the total influence or infection spread from the seed set S over*

the time interval $[t_0, t_0 + h]$, where each node v in S starts the infection process at time t_0 and can only influence other nodes while it is active.

The problem can be mathematically stated as:

$$\max_{S \subseteq V} \sigma(S, t_0, t_0 + h)$$

subject to the constraint that the seed set size $|S| \leq k$, where k is a predefined budget or capacity for selecting the seed nodes.

1.1 Our Contribution

Influence maximization in temporal networks presents significant challenges due to the dynamic nature of these networks and the complexity of diffusion processes. Traditional models often struggle with issues such as non-monotonicity and lack of submodularity in the spread function, especially when nodes cannot transit back to active states after recovery. This complexity complicates the process of optimal seed selection and increases computational costs [12] [13]. In this work, we contribute to the influence maximization on temporal social networks in the following ways:

- We establish that the spread function is non-monotone and submodular on temporal networks across any diffusion model featuring active-inactive transitions.
- We introduce cpSI-R, a novel diffusion model that ensures the monotonicity and submodularity of the objective function, thereby guaranteeing optimal seed selection quality.
- We enhance the forward influence algorithm by reducing computational costs, eliminating redundant computations, and implementing lazy forward optimization. This optimization leverages the submodular properties inherent in our diffusion model.
- We propose an improved sampling algorithm for efficiently sampling temporal snapshots, addressing both local and global structural similarities. We conduct comparative evaluations against four baselines, demonstrating significant performance improvements.

1.2 Organization of this article

The rest of the paper provides a brief overview of information diffusion models and their behaviour on temporal networks in Section 2 followed by an introduction of novel diffusion model cpSI-R under which the spread function is monotone submodular. In section 3 influence maximization under the cpSI-R model is discussed with all the related algorithms. Then, we provide the experimental results in section 4 and conclude with future work in section 5.

2 Information Diffusion

Information diffusion models on temporal networks study how information, behaviors, or diseases spread through networks that change over time, reflecting the dynamic nature of real-world interactions [14]. Temporal networks allow edges between nodes to appear and disappear, providing a more realistic representation of social interactions and communication patterns. Common diffusion models include the Independent Cascade (IC)

and Linear Threshold (LT) models, both adapted to temporal settings. These models often incorporate active-inactive transitions, where nodes can switch between influenced (active) and uninfluenced (inactive) states. However, under any diffusion model D that allows such transitions, the spread function $\sigma_D(S)$ is neither monotone nor submodular. This means that adding more nodes to the seed set does not always increase the spread, and the marginal gain from adding a node to the seed set can decrease as the seed set grows, due to the potential reversion of influenced nodes to an inactive state.

The lack of monotonicity and submodularity in the spread function presents significant challenges for designing efficient algorithms for influence maximization, as traditional greedy approaches rely on these properties for optimal performance guarantees. Temporal diffusion models thus demand innovative methods to effectively capture dynamic interactions and influence processes. This often involves exploring alternative formulations of the spread function or employing heuristic algorithms tailored to the temporal nature of the network. Additionally, these models provide valuable insights into real-world phenomena such as the rapid rise and fall of social media trends, the temporal clustering of disease outbreaks, and the intermittent nature of communication in dynamic environments. By incorporating temporal variability and active-inactive transitions, these models aim to offer a more nuanced understanding of how influence propagates in complex, evolving networks. We define the active-inactive transition as follows:

Definition 1. (Active-Inactive Transitions in Diffusion Models) Let $G = (V, E)$ represent a temporal network with nodes V and edges E , where each node $v \in V$ exists in one of two states—active or inactive. In diffusion models allowing active-inactive transitions, each node v may switch from an active state (influencing neighbors) to an inactive state (no longer influencing neighbors). Formally, let $s_v(t) \in \{0, 1\}$ denote the state of node v at time t , where $s_v(t) = 1$ indicates the active state and $s_v(t) = 0$ denotes the inactive state. The transition dynamics for each node v are defined as:

$$s_v(t_1) = 1 \quad \text{and} \quad s_v(t_2) = 0, \quad \text{for } t_1 < t_2 \Rightarrow s_v(t) = 0, \quad \forall t > t_2.$$

This implies that once a node transitions to the inactive state, it cannot return to the active state, thus making its influence spread temporary. As a result, the influence $\sigma(S)$ of a seed set $S \subseteq V$ becomes non-monotonic; adding more nodes to S does not necessarily increase the total influence spread because the duration of influence is constrained by the active state period of each node.

Lemma 1. The spread function $\sigma_D(S)$ is neither monotone nor submodular under any diffusion model that allows for the active-inactive transition.

Proof. We provide a counterexample as shown in Figure 1 for which the spread function is neither monotone nor submodular if there is a window for an activated node to become inactivated. Assume the probability of activation of a node b by node a at time t is 1, i.e., $p_{ab}^t = 1$. In this example, we have a temporal network T represented by snapshots T^1, T^2, T^3, T^4 .

Figure 1 shows the diffusion process when the seed set is $S = \{V_1^0\}$. Triangle-shaped nodes represent active or infected nodes at a given time t , round nodes represent those susceptible to infection in future time stamps greater than t , and rectangular nodes represent nodes that have undergone an active-inactive transition. The spread function $\sigma_D(S)$ calculates the number of nodes infected through the chain of activations until the last snapshot T^4 . The influence obtained by the spread function equals the total number of rectangular and triangular nodes in T^4 , yielding a resulting spread of $\sigma_D(\{V_1^0\}) = 6$.

Now, consider the addition of node V_3^0 to the seed set S . Figure 2 shows the diffusion process. The activation of node V_3 at time $t = 0$ causes node V_4 to be activated at $t = 1$, followed by the active-inactive transition

at $t = 2$, blocking the spread of infection to V_5 and other nodes connected by the path V_4V_5 . This premature activation of V_3 , leading to the early active-inactive transition of node V_4 , reduces the influence spread. As a result, the spread becomes $\sigma_D(\{V_1^0, V_3^0\}) = 4 < \sigma_D(\{V_1^0\})$, proving that $\sigma_D(S)$ is non-monotone.

We use a similar approach to demonstrate that σ_D is not submodular. Consider two sets $A = \{V_1^0\}$ and $B = \{V_1^0, V_3^0\}$, where $A \subset B$. Adding node V_8^0 to set A results in a total influence of 7, as shown in Figure 4. Adding the same node to set B yields a total spread of 8 (see Figure 5), i.e., $\sigma_D(B \cup \{V_8^0\}) = 8$. Thus, we have:

$$\sigma(A \cup \{V_8^0\}) - \sigma(A) = 7 - 6 = 1 \quad \text{and} \quad \sigma(B \cup \{V_8^0\}) - \sigma(B) = 8 - 4 = 4.$$

Since $A \subset B$, it follows that:

$$\sigma(A \cup x) - \sigma(A) \not\geq \sigma(B \cup x) - \sigma(B),$$

which violates the submodularity property.

We conclude that the spread function $\sigma_D(S)$ is neither monotone nor submodular in temporal networks where nodes exhibit recovery probability. This implies that there is no guarantee on the optimality gap for the solution obtained using a greedy algorithm under the IC, LT, or SIR models. However, for the SI model, we can still achieve a solution that is at most $1 - \frac{1}{e}$ times away from the optimal solution by applying a greedy method [1]. Additionally, computation costs can be reduced using lazy forward optimization [15] with the SI model on temporal networks. In the following subsection, we present an SI-like information diffusion model called the Continuous Persistent SI model with Reinforcement (cpSI-R). \square

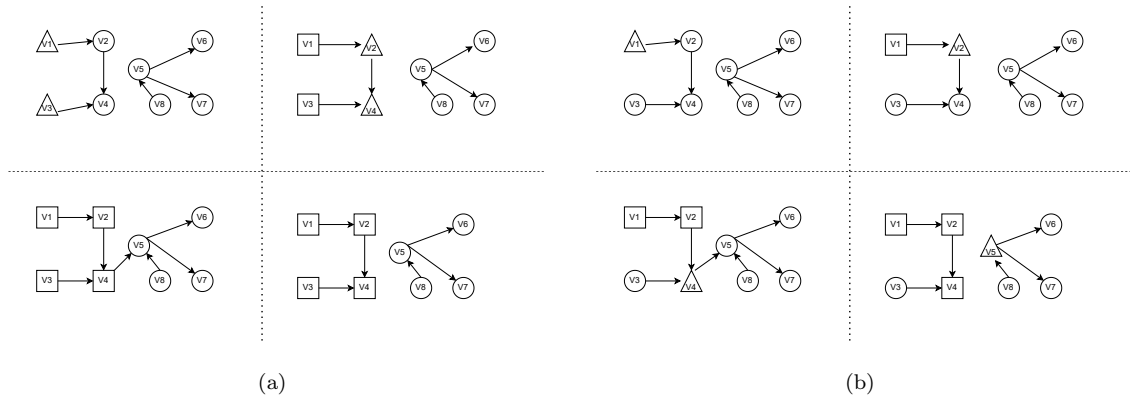


Figure 1: Counter example showing the violation of monotonicity under active-inactive transition (a): Seed set contains two infected nodes V_1 and V_3 (b): Seed set contains a single infection V_1

2.1 cpSI-R Model

In traditional diffusion models, influence spreads in a simplistic, often static manner, failing to capture the dynamic and temporal nuances of real-world interactions. Temporal social networks, however, are characterized by active-inactive transitions, where nodes do not continuously exert influence. Instead, their influence can fluctuate based on interaction patterns, time, and repeated exposures. These temporal dynamics are crucial in scenarios like behavioral change campaigns or viral marketing, where repeated interactions increase the likelihood of adoption but may diminish over time if not reinforced. Existing models lack mechanisms to simulate such persistent yet time-limited influence, leading to suboptimal or unrealistic predictions in dynamic networks.

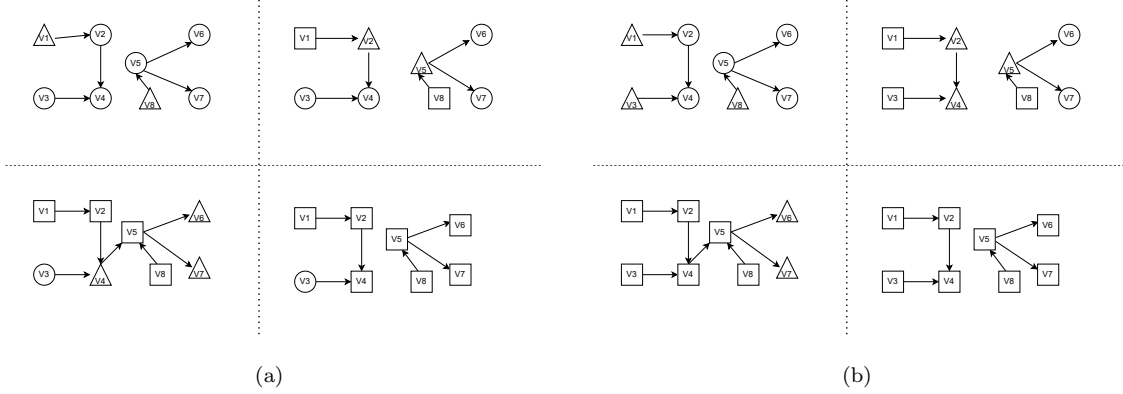


Figure 2: Counter example showing the violation of submodularity under active-inactive transition (a): Seed set contains one infected node V_1 and an additional node V_8 (b): Seed set contains V_1, V_3 and an additional node V_8

To address this gap, we introduce the Continuous Persistent Susceptible-Infected Model with Time-Limited Reinforcement and Re-activation (cpSI-R), specifically designed to reflect the persistence and decay of influence in temporal settings. This model describes a diffusion process where nodes (users) that become infected (adopt a behavior) continue to try to infect (influence) their neighbors within a designated time frame. If an infected node fails to spread the infection within this period, it loses its ability to influence others unless reactivated by interacting with another active node. The infection probability increases with each subsequent exposure, mirroring real-world situations where repeated interactions strengthen the likelihood of adoption.

A maximum time frame τ is introduced within which an infected node can spread the infection. If an infected node does not spread the infection within τ time units, it becomes inactive for spreading influence until reactivated by an active node. Let δ_u denote the time of the last infection attempt by node u . If $t_{uv}^k - \delta_u > \tau$, then node u becomes inactive for spreading the infection until reactivated. This captures scenarios like a social media fitness campaign, where users may be encouraged to adopt healthy habits through continuous exposure to fitness-related posts. Each time a user sees a fitness post, their likelihood of adopting the habit increases, with influence fluctuating over time based on interaction patterns. If users disengage from fitness content for an extended period, they lose the drive to influence others unless re-engaged by active users.

When a node u becomes infected at time t , it attempts to influence a susceptible node v based on a series of temporal exposures, represented by the sequence $\{t_{uv}^k\}_{k \geq 1}$ where an edge between u and v exists after time t . Each exposure increases the infection probability $p_{uv}(t_{uv}^k)$:

$$p_{uv}(t_{uv}^k) = p_0 \cdot (1 - e^{-\alpha k}) \cdot f(t_{uv}^k),$$

where p_0 is the base infection probability, α is a reinforcement factor, k is the exposure count, and $f(t_{uv}^k)$ is a temporal function adjusting the probability based on t_{uv}^k . At each t_{uv}^k , if v is susceptible, u tries to infect v with probability $p_{uv}(t_{uv}^k)$. If successful, v becomes infected, continuing the process from v .

The time-dependent influence is modeled by:

$$f(t_{uv}^k) = \beta e^{-\gamma(t_{uv}^k - t)},$$

where β is a scaling factor and γ controls the decay rate of influence over time.

Theorem 1. For any instance of the cpSI-R model on a temporal graph with fixed probabilities and a temporal interaction function, the spread function σ_{cpSI-R} is monotone and submodular.

Proof. We aim to demonstrate that the spread function σ_{cpSI-R} is both monotone and submodular.

Monotonicity: Let S represent the initial set of infected nodes, and consider a new set $S' = S \cup \{u\}$, where u is an additional node. The spread function $\sigma_{cpSI-R}(S)$ defines the expected number of nodes that become infected starting from the set S . When the node u is added to the set, it may infect new nodes that were not reachable from S alone, thereby increasing the total number of infected nodes. Consequently, the expected spread from S' must be at least as large as that from S , i.e.,

$$\sigma_{cpSI-R}(S') \geq \sigma_{cpSI-R}(S).$$

Thus, the spread function σ_{cpSI-R} is monotone.

Submodularity: Submodularity requires that the marginal gain from adding a node to a set decreases as the set grows. In formal terms, we need to show that for any $S \subseteq S'$ and any node u , the marginal increase in the spread function from adding u to S is at least as large as adding u to the superset S' . That is, we need to show:

$$\sigma_{cpSI-R}(S \cup \{u\}) - \sigma_{cpSI-R}(S) \geq \sigma_{cpSI-R}(S' \cup \{u\}) - \sigma_{cpSI-R}(S').$$

Consider the behavior of the cpSI-R model over time. At any time step t , the set of nodes that become active (infected) from S is the same as the set of nodes reachable from S . Now, consider the same diffusion process starting from the larger set S' . Since $S \subseteq S'$, all nodes that can be reached and activated from S are also reachable from S' , but S' may reach more nodes.

Thus, adding node u to the smaller set S can potentially activate a larger portion of nodes that were not reachable from S alone, whereas adding u to the larger set S' may lead to a smaller additional spread, as some of those nodes may already be reachable from S' without u . Hence, the marginal gain of adding u to S is at least as large as adding u to S' , which implies submodularity:

$$\sigma_{cpSI-R}(S \cup \{u\}) - \sigma_{cpSI-R}(S) \geq \sigma_{cpSI-R}(S' \cup \{u\}) - \sigma_{cpSI-R}(S').$$

Therefore, the spread function σ_{cpSI-R} is submodular.

Combining both results, we conclude that σ_{cpSI-R} is both monotone and submodular. \square

In our cpSI-R model, we extend the dynamics to incorporate time-limited interactions where nodes can transmit information only within specific time frames unless reactivated. The model captures diffusion dynamics with increasing infection probabilities due to repeated exposures, reflecting scenarios where repeated interactions or reinforcements increase the likelihood of adoption. Let's denote the node set of the network at time t as $V(t)$ and the edge set as $E(t)$, forming the dynamic graph $G(t) = (V(t), E(t))$.

Each edge (u, v) in $E(t)$ has a time-limited transmission probability $p_{uv}(t_1, t_2)$ over the interval (t_1, t_2) , where t_1 and t_2 are times within which the edge (u, v) is active. This probability is computed based on the periods δt_m when the edge is active.

3 Influence Maximization through cpSI-R

In the cpSI-R model, accurately assessing node influence over time intervals is essential for understanding diffusion dynamics. We introduce a method that discretizes time intervals based on both global and local

structural similarities. This approach ensures that time intervals align with significant network changes, thereby enhancing the fidelity of influence estimation.

Our contribution lies in refining the dynamic update equations within the cpSI-R framework and reducing the computational costs by eliminating the repetitive calculation of probability values of seeds across all iterations. These equations now incorporate time-dependent transmission probabilities derived from a sophisticated sampling algorithm that adapts to both global and local structural evolution. This adaptation not only improves computational efficiency but also enhances the model’s fidelity to real-world diffusion processes where network structures evolve dynamically. Moreover, by ensuring that the sampling captures critical changes in network topology, the model provides a robust framework for applications such as epidemic control, targeted marketing, and information dissemination in rapidly shifting environments. This nuanced understanding of dynamic influence equips decision-makers with precise tools for optimizing interventions in temporal settings.

Algorithm 1 TemporalInfluenceMaximization

Require: Transmission Matrix $F(\cdot)$, Time Horizon $(t_0, t_0 + h)$, Seed Set Size k , Temporal Network T , Maximum Time Stamp \max_t , Threshold η , Weighting Factors α, β , Minimum Iterations MinIter

Ensure: Set S of k influential nodes

- 1: $t_{\text{set}} \leftarrow \text{SamplingAlgorithm}(T, \max_t, \eta, \alpha, \beta)$ ▷ Step 1: Temporal Sampling
 - 2: **for** each node $i \in N(t_0)$ **do**
 - 3: $\text{CalcInfluence}(\{i\}, F(\cdot), (t_0, t_0 + h))$ ▷ Step 2: Initialize Influence Calculation
 - 4: **end for**
 - 5: $S \leftarrow \text{LazyForwardInfluence}(F(\cdot), (t_0, t_0 + h), k, \text{MinIter})$ ▷ Step 3: Lazy Forward Influence Maximization
 - 6: $\text{FinalInfluence} \leftarrow \text{CalcInfluence}(S, F(\cdot), (t_0, t_0 + h))$ ▷ Step 4: Final Influence Calculation for Selected Set S
 - 7: **return** S
-

Algorithm 2 CalcInfluence

Require: Seed Set S , Transmission Matrix $F(\cdot)$, Time Stamp $(t_0, t_0 + h)$

Ensure: Influence of seed set S

- 1: Initialize $p(i, t_0) = 1$ for each $i \in S$ and 0 otherwise
 - 2: Divide $(t_0, t_0 + h)$ into time periods $t_0, \dots, t_r = t_0 + h$ using *SamplingAlgorithm*
 - 3: $j \leftarrow 0$
 - 4: **repeat**
 - 5: Compute edge set $E(t_j, t_{j+1})$ and spread matrix $P(t_j, t_{j+1})$
 - 6: **for** each i **do**
 - 7: Compute $p(i, t_{j+1})$ using dynamic update equations for cpSI-R model
 - 8: **end for**
 - 9: $j \leftarrow j + 1$
 - 10: **until** $j = r$
 - 11: **return** $|S| + \sum_{i \in N(t)/S(t)} p(i, t_r)$
-

$\text{CalcInfluence}()$ initializes node influence probabilities based on the initial set S and discretizes the time interval $(t_0, t_0 + h)$ into intervals using the Sampling Algorithm given below that dynamically adjusts to structural changes in the network. It computes transmission probabilities and updates influence probabilities $p(i, t)$ iteratively using modified dynamic equations suited for the cpSI-R model. By focusing computations on active seeds only and integrating efficient sampling techniques, it minimizes computational overhead while maximizing accuracy in influence estimation.

The computational overhead is also reduced through effective sampling as oversampling adds to the cost whereas undersampling tells upon the quality of seeds. We provide a method to effectively sample the temporal network as follows:

We provide a sampling algorithm in which the goal is to partition time into smaller intervals that capture structural changes between consecutive graph snapshots. This partitioning is crucial for understanding how network properties evolve over time. Our sampling algorithm leverages two measures of structural similarity: Jaccard similarity $L(G_1, G_2)$ and Kulczynski similarity $K(G_1, G_2)$. We selected Jaccard and Kulczynski similarities for time partitioning because they offer a comprehensive view of how the network evolves both locally and globally. Jaccard similarity focuses on how much overlap exists between two snapshots by comparing the shared edges, which helps us track changes in direct connections or local structures in the network. Kulczynski similarity, however, goes further by also considering the individual edge sets of both snapshots, offering a broader perspective on how the network’s overall structure evolves over time. This combined approach ensures that we capture not just minor, localized changes, but also broader shifts in the network’s architecture. By using both of these complementary measures, we can more accurately identify the key moments when structural changes occur, which is crucial for calculating influence in a dynamic environment like the cpSI-R model.

Definition 2 (Jaccard Similarity). *Given two graph snapshots G_1 and G_2 , the Jaccard similarity $L(G_1, G_2)$ is defined as:*

$$L(G_1, G_2) = \frac{|E(G_1) \cap E(G_2)|}{|E(G_1) \cup E(G_2)|}$$

where $E(G)$ denotes the set of edges in graph G .

Definition 3 (Kulczynski Similarity). *Given two graph snapshots G_1 and G_2 , the Kulczynski similarity $K(G_1, G_2)$ is defined as:*

$$K(G_1, G_2) = \frac{1}{2} \left(\frac{|E(G_1) \cap E(G_2)|}{|E(G_1)|} + \frac{|E(G_1) \cap E(G_2)|}{|E(G_2)|} \right)$$

where $E(G)$ denotes the set of edges in graph G .

The cumulative score *Score* combines these similarities to determine whether to select a time stamp t :

$$Score = \alpha \cdot L(G_1, G_2) + \beta \cdot K(G_1, G_2)$$

where α and β are weighting factors controlling the influence of Jaccard and Kulczynski similarities, respectively.

While the efficient influence estimation is very important, it is crucial to determine the specific time intervals where the network’s structure evolves significantly. These intervals play a key role in improving accuracy without adding unnecessary computational overhead. This is where the Sampling Algorithm becomes essential.

3.1 Sampling Algorithm

The algorithm initiates by evaluating the structural similarity between successive graph snapshots G_1 and G_2 at each time stamp t . It computes *Score* using the combined metrics of Jaccard and Kulczynski similarities, adjusted by weighting factors α and β . If *Score* exceeds the threshold η , t is added to t_set and incremented. If not, it dynamically adjusts t using an exponential step size until significant structural changes are detected, ensuring that time stamps are selected based on substantial network evolution. This adaptive approach balances computational efficiency with the need to capture meaningful temporal dynamics in complex networks. This sampling strategy is designed to complement the *CalcInfluence()*, facilitating effective sampling of temporal networks and calculating the influence spread of seeds to capture influential nodes and their propagation dynamics over time. This approach facilitates robust analysis of temporal networks by identifying time intervals where structural changes are pronounced, enabling the optimal sampling strategy.

Although the Sampling Algorithm efficiently identifies key time intervals, determining the most influential nodes in a short span of time within those intervals is equally important. Without this, we cannot fully capture how influence propagates throughout the network. The next section addresses this by introducing the Lazy Forward Influence algorithm.

Algorithm 3 SamplingAlgorithm

Require: Temporal Network T , Maximum Time Stamp max.t , Threshold η , Weighting Factors α, β

Ensure: Set of selected time stamps t_{set}

```

1: Initialize empty set  $t_{\text{set}}$ 
2:  $t = 0$ 
3: while  $t \leq \text{max.t}$  do
4:    $G_1 \leftarrow \text{ObtainSnapshot}(T, t)$ 
5:    $G_2 \leftarrow \text{ObtainSnapshot}(T, t + 1)$ 
6:   Compute Score =  $\alpha \cdot L(G_1, G_2) + \beta \cdot G(G_1, G_2)$ 
7:   if Score  $\geq \eta$  then
8:     Add  $t$  to  $t_{\text{set}}$ 
9:      $t \leftarrow t + 1$ 
10:  else
11:     $step \leftarrow 1$ 
12:    while Score  $< \eta$  and  $t \leq \text{max.t}$  do
13:       $t \leftarrow t + step$ 
14:       $G_2 \leftarrow \text{ObtainSnapshot}(T, t)$ 
15:      Recalculate Score =  $\alpha \cdot L(G_1, G_2) + \beta \cdot G(G_1, G_2)$ 
16:       $step \leftarrow 2 \cdot step$ 
17:    end while
18:    if Score  $\geq \eta$  then
19:      Add  $t$  to  $t_{\text{set}}$ 
20:       $t \leftarrow t + 1$ 
21:    else
22:       $t \leftarrow t + step$ 
23:    end if
24:  end if
25: end while
26: return  $t_{\text{set}}$ 

```

3.2 Lazy Forward Influence

We introduce the *LazyForwardInfluence* algorithm, which leverages lazy forward optimization [16] to identify influential nodes in a temporal network. This method eliminates the exhaustive step of evaluating each node in $N(t_0) - S$ for potential replacement with any node in S . Instead, it incorporates a mechanism to track iterations without replacements and terminates early if no replacements occur for a specified number of iterations. This approach significantly reduces computational overhead while preserving seed quality, ensuring an efficient and effective analysis of temporal network dynamics.

The *LazyForwardInfluence* algorithm starts by computing the influence values for all nodes at the initial time point t_0 using the *CalcInfluence* function. It then selects an initial set S of k nodes with the highest influence values. A priority queue (max-heap) is created to store the nodes in $N(t_0) - S$ sorted by their influence values. The algorithm proceeds iteratively, extracting the node with the highest influence from the priority queue and evaluating potential replacements for nodes in S .

During each iteration, the algorithm identifies the node i from the priority queue and evaluates the potential influence gain for replacing each node j in S . If a beneficial replacement is found, the nodes are swapped, and

the counter *NoReplace* is reset. If no replacements occur, the counter increments. If *NoReplace* reaches the predefined threshold (*MinIter*), the algorithm terminates early, returning the current set *S*.

This method enhances efficiency by avoiding unnecessary evaluations through lazy forward optimization. It dynamically adjusts the set of influential nodes based on observed influence gains, balancing computational efficiency with the quality of the selected seeds, and providing an optimal sampling strategy in evolving temporal networks. With the mechanisms for identifying key time intervals and influential nodes in place, it is important

Algorithm 4 LazyForwardInfluence

Require: Transmission Matrix $F(\cdot)$, Time Horizon $(t_0, t_0 + h)$, Number of Influence Points k , Minimum Iterations *MinIter*

Ensure: Set *S* of k influential nodes

```

1: for each node  $i \in N(t_0)$  do
2:   Compute CalcInfluence( $\{i\}, F(\cdot), (t_0, t_0 + h)$ )
3: end for
4:  $S \leftarrow$  initial set of  $k$  nodes with the highest CalcInfluence values
5: PriorityQueue  $\leftarrow$  initialize max-heap with nodes in  $N(t_0) - S$  ordered by CalcInfluence value
6: NoReplace  $\leftarrow 0$ 
7: while NoReplace < MinIter and PriorityQueue.isEmpty() = false do
8:    $i \leftarrow$  PriorityQueue.extractMax()
9:   maxIncrease  $\leftarrow 0$ 
10:  replaceNode  $\leftarrow$  null
11:  for each node  $j \in S$  do
12:    influenceGain  $\leftarrow$  CalcInfluence( $S \cup \{i\} - \{j\}, F(\cdot), (t_0, t_0 + h)$ ) - CalcInfluence( $S, F(\cdot), (t_0, t_0 + h)$ )
13:    if influenceGain > maxIncrease then
14:      maxIncrease  $\leftarrow$  influenceGain
15:      replaceNode  $\leftarrow j$ 
16:    end if
17:  end for
18:  if replaceNode  $\neq$  null and maxIncrease > 0 then
19:     $S \leftarrow S \cup \{i\} - \{\text{replaceNode}\}$ 
20:    NoReplace  $\leftarrow 0$ 
21:  else
22:    NoReplace  $\leftarrow$  NoReplace + 1
23:  end if
24: end while
25: return  $S$ 

```

to illustrate the practical utility of these algorithms. A toy example on a temporal network will demonstrate the effectiveness of the cpSI-R model and the associated algorithms in capturing influence dynamics over time. To illustrate the working of the cpSI-R model and the algorithms, we assume a toy temporal network as shown in Figure 3.

We begin by allowing the network to evolve in one direction, where edges are added over time, while deletions are restricted for simplicity. This ensures that we study the diffusion process in a setting where network complexity gradually increases. A key component of our approach is the sampling algorithm, which partitions time into intervals based on structural similarity between consecutive snapshots. We chose $\eta = 0.3$, which leads to the selection of snapshots 1, 2, 4, and 8 based on their similarity scores, drastically reducing computational time. For example, if selecting all snapshots required $O(T)$ computations where T is the total number of snapshots, selecting fewer snapshots based on η reduces this to $O(\eta T)$, offering computational efficiency, particularly when η is on the higher side. The similarity score is calculated as:

$$\text{Score}(G_1, G_2) = \alpha \cdot L(G_1, G_2) + \beta \cdot K(G_1, G_2)$$

where $L(G_1, G_2)$ is the Jaccard similarity defined as:

$$L(G_1, G_2) = \frac{|E(G_1) \cap E(G_2)|}{|E(G_1) \cup E(G_2)|}$$

and $K(G_1, G_2)$ is the Kulczynski similarity:

$$K(G_1, G_2) = \frac{1}{2} \left(\frac{|E(G_1) \cap E(G_2)|}{|E(G_1)|} + \frac{|E(G_1) \cap E(G_2)|}{|E(G_2)|} \right)$$

In our case, $\alpha = 0.5$ and $\beta = 0.5$, giving equal weight to both similarities. For example, in our toy temporal network between two snapshots at $t = 1$ and $t = 2$ represented as G_1^1 and G_2^2 respectively, the number of common edges $|E(G_1^1) \cap E(G_2^2)| = 1$, $|E(G_1^1)| = 1$, and $|E(G_2^2)| = 4$, the Jaccard similarity would be:

$$L(G_1, G_2) = \frac{4}{1 + 4 - 1} = \frac{1}{4} = 0.25$$

and the Kulczynski similarity would be:

$$K(G_1, G_2) = \frac{1}{2} \left(\frac{1}{1} + \frac{1}{4} \right) = \frac{1}{2} (1 + 0.25) = 0.6$$

Thus, the overall similarity score is:

$$\text{Score}(G_1, G_2) = 0.5 \cdot 0.25 + 0.5 \cdot 0.6 = 0.4$$

Since the score exceeds $\eta = 0.3$, the snapshot 2 is selected. Similarly snapshots 4, and 8 are selected and hence we significantly reduce computation time by focusing on only few snapshots instead of all.

Next, we calculate the influence of each node. Initially, for each node i , the influence probability $p(i, t_0)$ is set to 1 for seed nodes and 0 otherwise. For each time interval $[t_j, t_{j+1}]$, we compute the edge set $E(t_j, t_{j+1})$ and update the influence probabilities using the cpSI-R dynamic equations. For instance, if node 2 is a seed, its influence at time t_j is updated based on the spread matrix $P(t_j, t_{j+1})$, reflecting the probabilities of infecting its neighbors. After calculating individual node influences, we apply the Lazy Forward Influence algorithm to select the top k seed nodes, which maximizes the marginal gain in influence. In our toy network, we set $k = 2$, and after running the algorithm, nodes 2 and 3 emerge as the top seeds based on their cumulative influence.

The Lazy Forward Influence algorithm starts by calculating the influence of all nodes at the initial time point t_0 and constructs a priority queue of nodes based on their influence values. As the algorithm progresses, we iteratively update the seed set S to include nodes that offer the highest marginal gain. The influence of the final seed set S is computed as:

$$\text{Final Influence}(S) = |S| + \sum_{i \in N(t) \setminus S(t)} p(i, t_r)$$

where $p(i, t_r)$ represents the influence probability of non-seed nodes at the final time stamp t_r .

This approach not only reduces computational overhead but ensures accurate selection of influential nodes while capturing meaningful structural changes in the temporal network, resulting in nodes 2 and 3 being identified as the most influential. This is further demonstrated in the results section, where the optimal seed sets and influence spread are compared across different values of η and other parameters.

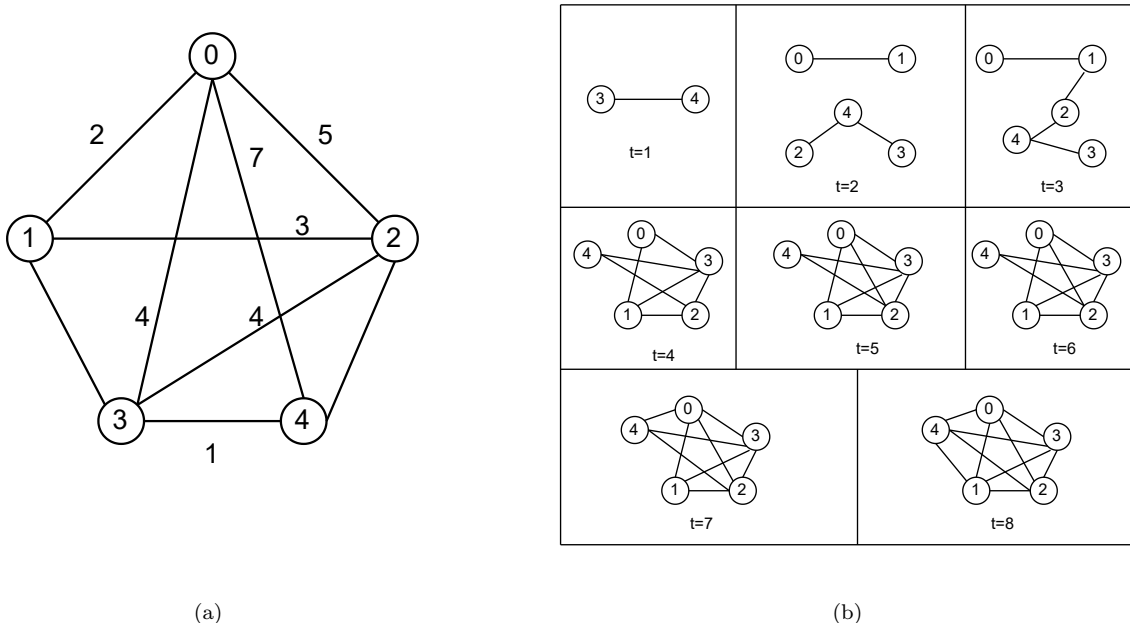


Figure 3: Example illustrating the working of cpSI-R model (a): Toy temporal network represented with initial contact sequences (b): Snapshots showing temporal evolution of a toy temporal network

4 Experiments

We run experiments on two real data sets in order to highlight the effectiveness of our approach. The experiments were run on a Windows system equipped with an Intel(R) Core(TM) i7-10875H CPU, 16 GB of RAM, and a 512 GB hard drive (Dell). All code was developed in PyCharm using Python 3.11.

4.1 Datasets

We used two data sets in order to test the approach.

Primary school temporal network data [17] [18]: The temporal interactions between students and teachers are captured in this dataset. Many lines with the same timestamp indicate multiple encounters in the same span. Seconds are used to measure time. There are 125,775 edges and 242 nodes in the dataset . More details are given in table 1.

Contact patterns in a village in rural Malawi [19]: This dataset contains the contact patterns in a village in rural Malawi, based on proximity sensors technology. More details are given in table 1

4.2 Implementation and Baselines

We calculate the seed set using *CalcInfluence()*, then utilize *SamplingAlgorithm()* to determine the sampled time stamps, and finally apply *TemporalInfluenceMaximization()* to calculate the influence of the seed set. Our approach relies on the sampling of temporal data to enhance accuracy in capturing influence maximization. We measured the influence across different sampling rates and determined the optimal values in both datasets. This choice balances the trade-off between computational feasibility and the accuracy of influence estimation. We chose the sampling parameter η values of 0.7 and 0.6 on Primary school dataset and Rural Malawi dataset

Table 1: Datasets Used for Testing

Dataset	Description
Primary School Temporal Network Data	<p>Temporal interactions between students and teachers, captured in a tab-separated list at 20-second intervals. Each entry is of the form “t, i, j, C_i, C_j” where:</p> <ul style="list-style-type: none"> • i and j: Anonymous IDs of participants • C_i and C_j: Respective courses of participants • Active interval: [t - 20s, t] • Contains 125,775 edges and 242 nodes.
Contact Patterns in a Village in Rural Malawi	<p>Contact patterns based on proximity sensors technology. Data collection was conducted from 16th December 2019 to 10th January 2020 in Mdoliro village, Dowa district, Malawi.</p> <ul style="list-style-type: none"> • Estimated population (2019): 147 • Distributed over 32 households (average household size: 4.5) • Contains 65,775 edges and 147 nodes

respectively because empirical validation showed these values effectively capture significant structural changes in temporal networks without oversampling or undersampling. Additionally, we select $\alpha = 0.5$ and $\beta = 0.5$ to give equal importance to both local and global similarity.

We compared the performance of our approach with the following baselines:

- **Dynamic Degree Discount [20]**: The algorithm selects influential seed nodes in a dynamic network over a time period using a susceptibility parameter α . The seed set is initially empty. Each node j is assigned an initial degree discount value $\Delta_j = \mathcal{D}_{\mathcal{T}}(j)$ and a time counter $\tau_j = 0$. During each iteration, the node with the highest Δ_j is added to the seed set. For each neighbor q of this node, the degree discount and time counter are updated as $\tau_q = \tau_q + 1$ and $\Delta_q = \mathcal{D}_{\mathcal{T}}(q) - 2\tau_q - (\mathcal{D}_{\mathcal{T}}(q) - \tau_q)\tau_q\alpha$. The algorithm continues until the seed set reaches the desired size. We have chosen the value of $\alpha = 0.01$ in our experiments.
- **Borgs and Tangs Algorithm [21] [22]**: This method by Borgs and Tang aims to identify influential seed nodes in a fixed network \mathcal{N} . The algorithm starts by selecting a node w at random and removing edges from \mathcal{N} with probability $1 - \lambda$, where λ is the susceptibility parameter. Afterward, it gathers nodes that are still reachable from w , forming a set of reachable nodes \mathcal{R} . This process is repeated γ times. The node with the highest frequency in \mathcal{R} is added to the seed set \mathcal{S} . The procedure continues until the size of \mathcal{S} reaches k . In our experiments, we have chosen the value of susceptibility as 0.01
- **Dynamic CI [20]**: Dynamic CI expands Morone’s method to dynamic networks by redefining node degrees and distances over time. The Dynamic CI index, $D_{\Theta_m}(x)$, is calculated as:

$$D_{\Theta_m}(x) = \Gamma(x) \sum_{y \in \Delta(x, m)} \Gamma(y)$$

where $\Gamma(x)$ is the dynamic degree of node x , and $\Delta(x, m)$ represents the set of nodes reachable from x within a minimum time of m . This index helps identify the top k influential nodes. Since it is difficult to perform experiments on taking different values of m , we have used $m = 10$ in our experiments.

- **Forward Influence Algorithm [11]:** The forward influence algorithm identifies influential nodes by first computing $\text{DynInfluenceVal}(\{i\}, F(\cdot), (t_0, t_0 + h))$ for each node $i \in N(t_0)$ and selecting the top k nodes. It then iteratively replaces nodes in this set with others to maximize the increase in influence, evaluating changes as $\text{DynInfluenceVal}(S \cup \{i\} \setminus \{j\}, F(\cdot), (t_0, t_0 + h)) - \text{DynInfluenceVal}(S, F(\cdot), (t_0, t_0 + h))$. The process continues until no significant improvement is found or a maximum number of iterations is reached.

4.3 Results and Analysis

We present the outcomes of influence spread across various seed sizes (k) and sampling parameter values (η) in two datasets: Primary School and Rural Malawi, as shown in Figure 4(a) and 4(b) respectively. In these figures, the x -axis represents the seed set size as a percentage of the total nodes ($\frac{k}{|V|} \times 100$), while the y -axis reflects the percentage of influenced nodes. The analysis highlights how varying η impacts both influence spread and computational efficiency, showcasing notable differences in algorithm performance.

In our experiments, we varied η to sample temporal snapshots, balancing the trade-off between influence spread and running time. Lower values of η tend to result in better influence spread, while higher values provide faster computation times. In the Primary School dataset, our proposed cpSI-R algorithm consistently outperforms baseline algorithms. At $\eta = 0.4$, cpSI-R begins to lead in influence spread and becomes significantly stronger at $\eta = 0.7$. However, as we increase η to 0.7, the infection spread decreases, and the performance of our algorithm aligns more closely with the forward influence algorithms. Additionally, decreasing η increases the time taken to select the seed nodes, as it requires more snapshots. This presents a trade-off between seed quality and time efficiency. As seed size increases, our algorithm continues to surpass Borgs and Tang’s Algorithm, Dynamic Degree Discount, Dynamic CI, and the Forward Influence Algorithm. The forward influence algorithm also achieves a substantial infection rate but requires more computational resources compared to our algorithm. The pattern in figures 4(a) and 5(a) reveals the efficiency in our algorithm as it delivers high infection rate with less computation time. This highlights the ability of cpSI-R to efficiently balance diffusion quality and speed, especially at higher η values, improving performance both in terms of spread and computational time.

A similar trend is observed on Rural malawi dataset where our algorithm demonstrates highest percentage of infected nodes across all seed sizes particularly excelling as seed size increases indicating more robustness in achieving higher spread under temporal dynamics. The Borgs and Tangs Algorithm, while efficient in computation, results in lower infection spread compared to other methods. Dynamic Degree Discount and Dynamic Collective Influence (CI) algorithms provide intermediate performance, balancing infection spread with computational efficiency, though they trail behind our algorithm in maximizing infection percentage. Despite the unique challenges of the Rural Malawi network, cpSI-R adapts effectively, consistently infecting a larger percentage of nodes as the seed size increases. Its performance at $\eta = 0.6$ demonstrates its ability to scale efficiently while maintaining competitive influence spread, even in complex network structures.

Theoretically, the cpSI-R model leverages temporal network dynamics, where the probability of infection varies over time, capturing the probabilistic nature of influence based on repeated exposures. By incorporating reinforcement and reactivation, cpSI-R theoretically supports a higher degree of influence spread due to its

dynamic reinforcement mechanism. The use of η as a sampling parameter enables theoretical tuning of diffusion quality in temporal networks, aligning with the submodular properties of cpSI-R and providing a mathematically grounded way to control the trade-off between influence spread and computational expense. As η increases, the model samples fewer snapshots, reducing the computational load; however, theoretically, this may reduce the robustness of influence spread since fewer time points capture network interactions. By contrast, smaller values of η capture more snapshots, enhancing the influence spread but increasing computational costs, consistent with submodular optimization principles

A key challenge is resolving the trade-off between influence spread and computational efficiency. Based on our results, we identified optimal values of η for both datasets. For the Primary School dataset, these are $\eta = 0.4$ and $\eta = 0.7$, while for the Rural Malawi dataset, $\eta = 0.5$ and $\eta = 0.6$ are the most effective. These values strike a balance, minimizing computational costs without significantly compromising influence spread. The plots illustrate that at these critical points, cpSI-R achieves superior performance in both datasets, demonstrating its robustness and flexibility.

4.4 Discussion

The cpSI-R model effectively addresses the challenges of influence maximization in temporal social networks by incorporating persistent influence and node reactivation mechanisms. These enhancements are particularly impactful in scenarios where network relationships undergo frequent active-inactive transitions, such as political campaigns and health interventions. The model’s ability to maintain monotonicity and submodularity ensures computational efficiency, as evidenced by its superior performance across multiple datasets.

Results demonstrate that cpSI-R achieves a high influence spread while minimizing computational costs. For instance, the experiments on the Primary School dataset highlight that η values of 0.4 and 0.7 optimize the trade-off between computational efficiency and diffusion quality. Similarly, in the Rural Malawi dataset, cpSI-R exhibits robust performance, particularly at $\eta = 0.5$ and $\eta = 0.6$, indicating its adaptability to varied network topologies. The theoretical properties of cpSI-R align with its practical outcomes, supporting the notion that strategic sampling of temporal snapshots can preserve influence quality while managing computational overhead.

The findings underscore the resilience and scalability of cpSI-R, which is critical for real-world applications. Its performance across dense and sparse networks validates its versatility, making it suitable for a wide range of domains, including marketing, epidemic control, and opinion dynamics. However, the inherent trade-off between influence spread and computational efficiency remains a key challenge, necessitating further exploration of dynamic and adaptive strategies to optimize performance under evolving network conditions.

η	%age of infected nodes	Time(sec)
0.1	89	5900
0.2	88	5700
0.3	87	5700
0.4	87	5500
0.5	86	5400
0.6	85	5300
0.7	84	5100
0.8	81	5100
0.9	80	4800

Figure 4: Performance of the model on the Primary School dataset, presenting the correlation between η (snapshot sampling parameter), the percentage of infected nodes, and the time taken in seconds with the optimal value of η highlighted

η	%age of infected nodes	Time(sec)
0.1	88	3700
0.2	86	3700
0.3	86	3700
0.4	86	3400
0.5	86	3400
0.6	86	3200
0.7	85	3200
0.8	84	3000
0.9	84	2900

Figure 5: Performance of the model on the the RM dataset, presenting the correlation between η (snapshot sampling parameter), the percentage of infected nodes, and the time taken in seconds with the optimal value of η highlighted

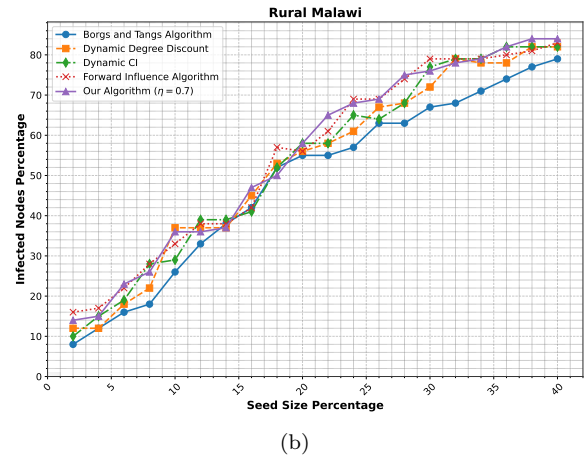
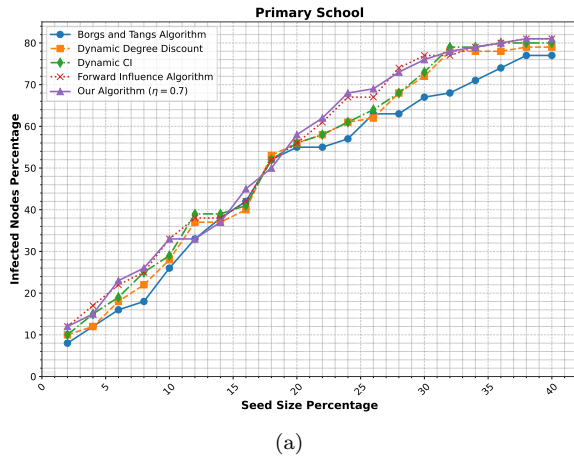
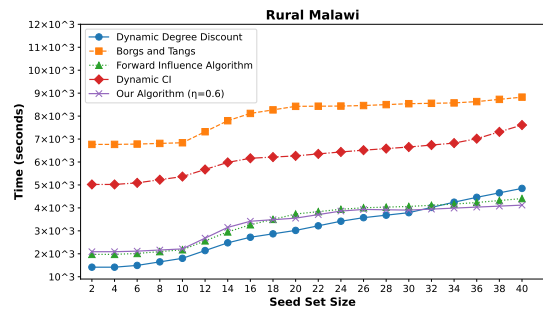
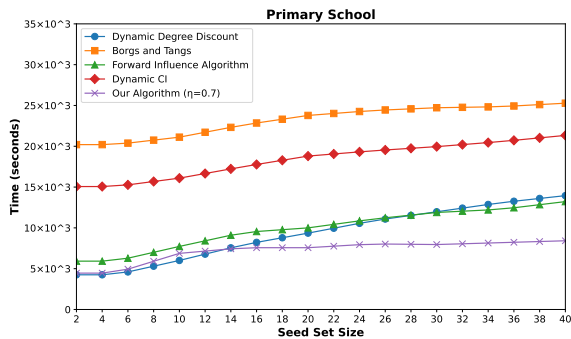


Figure 6: Results for percentage infection spread with varying seed size on the (a): Primary School dataset with value of $\eta = 0.7$ in our algorithm, (b): Rural Malawi dataset with value of $\eta = 0.6$ in our algorithm



(a) Primary school dataset with value of $\eta = 0.7$ in our algorithm

(b) Rural Malawi dataset with value of $\eta = 0.6$ in our algorithm

Figure 7: Efficiency Results for (a) Primary school dataset with value of $\eta = 0.7$ in our algorithm, and (b) Rural Malawi dataset with value of $\eta = 0.6$.

5 Conclusion and Future Work

The cpSI-R model marks a substantial advancement in influence maximization on temporal social networks, adeptly capturing the complexities of dynamic interactions. By integrating persistent influence and reactivation mechanisms, it bridges critical gaps in traditional diffusion models, enabling a more accurate representation of real-world network behavior. The model’s ability to maintain monotonicity and submodularity enhances its optimization capabilities, as demonstrated by its superior performance across both dense and sparse network structures. Experimental results, particularly at optimal η values, highlight its ability to achieve a high influence spread while balancing computational efficiency. This balance, achieved through selective temporal snapshot sampling, underscores the practical utility of cpSI-R for applications requiring both scalability and precision, such as marketing campaigns, health interventions, and political mobilization.

Looking to the future, the cpSI-R model presents several promising avenues for research and development. Enhancing its adaptability to more diverse temporal network configurations will allow for a deeper understanding of influence dynamics across various contexts, including networks with heterogeneous interaction patterns. Further exploration into adaptive strategies that respond to real-time network fluctuations could enable the model to better capture the evolving nature of social interactions. Scaling the model to accommodate large, complex networks will be a priority, leveraging parallel processing and approximation techniques to ensure computational feasibility. Expanding its application to domains such as epidemic control, opinion dynamics, and real-time marketing will test its robustness in diverse environments. Collaborative efforts across disciplines, integrating insights from sociology, behavioral science, and computational research, will refine the model further, driving both theoretical innovation and practical impact in influence maximization challenges.

References

- [1] D. Kempe, J. Kleinberg, and E. Tardos, “Maximizing the spread of influence through a social network,” in *Proceedings of the Ninth ACM SIGKDD International Conference on Knowledge Discovery and Data Mining*, KDD ’03, (New York, NY, USA), p. 137–146, Association for Computing Machinery, 2003.
- [2] J. Leskovec, L. A. Adamic, and B. A. Huberman, “The dynamics of viral marketing,” *ACM Trans. Web*, vol. 1, no. 1, p. 5–es, 2007.
- [3] G. Tong, W. Wu, S. Tang, and D.-Z. Du, “Adaptive influence maximization in dynamic social networks,” *IEEE/ACM Trans. Netw.*, vol. 25, no. 1, p. 112–125, 2017.
- [4] W. Chen, C. Wang, and Y. Wang, “Scalable influence maximization for prevalent viral marketing in large-scale social networks,” in *Proceedings of the 16th ACM SIGKDD International Conference on Knowledge Discovery and Data Mining*, KDD ’10, (New York, NY, USA), p. 1029–1038, Association for Computing Machinery, 2010.
- [5] A. Zahoor, I. A. Gillani, and J. Bashir, “Tbcelf: Temporal budget-aware influence maximization,” in *Proceedings of the 7th Joint International Conference on Data Science & Management of Data (11th ACM IKDD CODS and 29th COMAD)*, CODS-COMAD ’24, (New York, NY, USA), p. 580–581, Association for Computing Machinery, 2024.
- [6] G. Song, Y. Li, X. Chen, X. He, and J. Tang, “Influential node tracking on dynamic social network: An interchange greedy approach,” *IEEE Transactions on Knowledge and Data Engineering*, vol. 29, no. 2, pp. 359–372, 2017.
- [7] W. Chen, Y. Wang, and Y. Yuan, “Combinatorial multi-armed bandit: general framework, results and applications,” in *Proceedings of the 30th International Conference on International Conference on Machine Learning - Volume 28*, ICML’13, p. I–151–I–159, JMLR.org, 2013.
- [8] S. Vaswani, B. Kveton, Z. Wen, M. Ghavamzadeh, L. V. S. Lakshmanan, and M. Schmidt, “Model-independent online learning for influence maximization,” in *Proceedings of the 34th International Conference on Machine Learning* (D. Precup and Y. W. Teh, eds.), vol. 70 of *Proceedings of Machine Learning Research*, pp. 3530–3539, PMLR, 2017.
- [9] Z. Wen, B. Kveton, M. Valko, and S. Vaswani, “Online influence maximization under independent cascade model with semi-bandit feedback,” 2018.
- [10] J. Zuo, X. Liu, C. Joe-Wong, J. C. S. Lui, and W. Chen, “Online competitive influence maximization,” in *Proceedings of The 25th International Conference on Artificial Intelligence and Statistics* (G. Camps-Valls, F. J. R. Ruiz, and I. Valera, eds.), vol. 151 of *Proceedings of Machine Learning Research*, pp. 11472–11502, PMLR, 2022.
- [11] C. C. Aggarwal, S. Lin, and P. S. Yu, *On Influential Node Discovery in Dynamic Social Networks*, pp. 636–647. SIAM, 2021.
- [12] M. Azaouzi, W. Mnasri, and L. B. Romdhane, “New trends in influence maximization models,” *Computer Science Review*, vol. 40, p. 100393, 2021.
- [13] S. Aral and P. S. Dhillon, “Social influence maximization under empirical influence models,” *Nature human behaviour*, vol. 2, no. 6, pp. 375–382, 2018.

- [14] P. Holme and J. Saramäki, “Temporal networks,” *Physics Reports*, vol. 519, p. 97–125, Oct. 2012.
- [15] J. Lv, J. Guo, Z. Yang, W. Zhang, and A. Jocshi, “Improved algorithms of celf and celf++ for influence maximization.,” *Journal of Engineering Science & Technology Review*, vol. 7, no. 3, 2014.
- [16] J. Leskovec, A. Krause, C. Guestrin, C. Faloutsos, J. VanBriesen, and N. Glance, “Cost-effective outbreak detection in networks,” in *Proceedings of the 13th ACM SIGKDD International Conference on Knowledge Discovery and Data Mining*, KDD '07, (New York, NY, USA), p. 420–429, Association for Computing Machinery, 2007.
- [17] V. Gemmetto, A. Barrat, and C. Cattuto, “Mitigation of infectious disease at school: targeted class closure vs school closure,” *BMC infectious diseases*, vol. 14, pp. 1–10, 2014.
- [18] J. Stehlé, N. Voirin, A. Barrat, C. Cattuto, L. Isella, J.-F. Pinton, M. Quaggiotto, W. Van den Broeck, C. Régis, B. Lina, *et al.*, “High-resolution measurements of face-to-face contact patterns in a primary school,” *PloS one*, vol. 6, no. 8, p. e23176, 2011.
- [19] L. Ozella, D. Paolotti, G. Lichand, J. P. Rodríguez, S. Haenni, J. Phuka, O. B. Leal-Neto, and C. Cattuto, “Using wearable proximity sensors to characterize social contact patterns in a village of rural malawi,” *EPJ Data Science*, vol. 10, no. 1, p. 46, 2021.
- [20] T. Murata and H. Koga, “Extended methods for influence maximization in dynamic networks,” *Computational social networks*, vol. 5, pp. 1–21, 2018.
- [21] C. Borgs, M. Brautbar, J. Chayes, and B. Lucier, “Maximizing social influence in nearly optimal time,” in *Proceedings of the twenty-fifth annual ACM-SIAM symposium on Discrete algorithms*, pp. 946–957, SIAM, 2014.
- [22] Y. Tang, X. Xiao, and Y. Shi, “Influence maximization: Near-optimal time complexity meets practical efficiency,” in *Proceedings of the 2014 ACM SIGMOD international conference on Management of data*, pp. 75–86, 2014.